Role of the strengthened El Niño teleconnection in the May 2015 floods over the southern Great Plains

S.-Y. Simon Wang[1,2*], Wan-Ru Huang[3], Huang-Hsiung Hsu[4], and Robert Gillies[1,2]

[1]Utah Climate Center, Utah State University, Logan, UT, USA
[2]Department of Plants, Soils, and Climate, Utah State University, Logan, UT, USA
[3]Department of Earth Sciences, National Taiwan Normal University, Taipei, Taiwan
[4]Research Center for Environmental Changes, Academia Sinica, Taipei, Taiwan

*Corresponding author: simon.wang@usu.edu, 4820 Old Main Hill, Logan UT 84322.

This article has been accepted for publication and undergone full peer review but has not been through the copyediting, typesetting, pagination and proofreading process which may lead to differences between this version and the Version of Record. Please cite this article as doi: 10.1002/2015GL065211

Abstract

The climate anomalies leading to the May 2015 floods in Texas and Oklahoma were analyzed in the context of El Niño teleconnection in a warmer climate. El Niño tends to increase late-spring precipitation in the southern Great Plains and this effect has intensified since 1980. There was a detectable effect of anthropogenic global warming in the physical processes that caused the persistent precipitation in May of 2015: Warming in the tropical Pacific acted to strengthen the teleconnection towards North America, modification of zonal wave-5 circulation that deepened the anomalous trough to the west of Texas, and an enhanced Great Plains low-level southerlies increasing moisture supply from the Gulf of Mexico. Attribution analysis using the CMIP5 single-forcing experiments and the CESM Large Ensemble Project indicated a significant increase in the El Niño-induced precipitation anomalies over Texas and Oklahoma when increases in the anthropogenic greenhouse gases were taken into account.

1. Introduction

In May of 2015, an El Niño had developed fully (Fig. 1a) and as a consequence – at least in part – precipitation anomalies in Texas and Oklahoma were off the scale reaching over 400 mm above normal (Fig. 1b); this was accompanied by dry anomalies in Kentucky and Tennessee. As the Texas news media echoed: "enough rain fell in May to cover the entire state 8 inches deep" (CNN 6/1/2015)[1] and in Houston alone, the flood damage was estimated to "top $45 million" (Associate Press 5/31/2015)[2]. While seasonal predictions, issued as early as March, had indicated increased May precipitation for the southern Great Plains[3], the extreme magnitude of the rainfall was not indicated nor anticipated – a challenge that is yet to be realized.

It is known that either the onset or a persistent El Niño can increase spring precipitation in the southern Great Plains while at the same time reducing precipitation in the southeast U.S. (e.g., Ropelewski and Halpert 1986, 1987; Lee et al. 2014b). Previous studies (e.g., Meehl and Teng 2007; Stevenson et al. 2012; Wang et al. 2014) have found that in a warmer climate, the teleconnection that underlies the El Niño-Southern Oscillation (ENSO) and its associated impact on North America would change in terms of intensification and/or a positional shift of the resultant climate anomalies; this regardless of the direction of future change in frequency and intensity that ENSO might take. Climate modifications that involve ENSO have forecast implications at both seasonal (Mo 2010) and decadal (Meehl et al. 2014) timescales, and it is reasonable to question to what extent, if any, the rather extreme May 2015 precipitation event that occurred during an El Niño was induced through a warming climate. It is therefore

[1] http://edition.cnn.com/2015/05/31/us/severe-weather/
[2] http://www.sltrib.com/news/2572138-155/story.html
[3] http://www.cpc.ncep.noaa.gov/products/NMME/

worthwhile to conduct a climate diagnostics and an attribution analysis of the May 2015 high-precipitation event that occurred over Texas and Oklahoma.

2. Data

In our analysis, we adopted 17 models from the Coupled Model Intercomparison Project Phase 5's (CMIP5) Historical single-forcing experiments that were driven by (1) natural-only forcing including solar and volcano (NAT), (2) greenhouse gas (GHG)-only forcing, and (3) all these historical forcings (ALL) including anthropogenic aerosols (Taylor et al. 2011). Each experiment produced multiple members initialized from a long-stable preindustrial (1850) control run up to 2005. Table S1 provides the full name, institute, ensemble size, and spatial resolution of these models[4]. In addition, we utilized 30 members produced by the Community Earth System Model version 1 (CESM1) through the Large Ensemble Project (LEP; Kay et al. 2014). The CESM1 ensemble simulations covered two periods: 1920-2005 with "ALL" forcing and 2006-2080 with RCP8.5 forcing (the range of radiative forcing increase at 8.5 W/m^2 per year till the year 2100 relative to pre-industrial values). The CESM1 was used here because it simulates well the ENSO cycle and associated teleconnection in North America (Wang et al. 2014; Wang et al. 2015). All model outputs were re-gridded to 2.5° longitude × 2.5° latitude resolution before averaging, to be comparable with the NCEP/NCAR Reanalysis (R1) data (Kalnay et al. 1996). Although the R1 is an older-generation reanalysis, it is the only dataset that covers the pre-satellite era (before 1979) and yet is still updated operationally. Meanwhile, we utilized four satellite-era reanalyses to establish a consensus for the trend analysis, including MERRA (Rienecker et al. 2011),

[4] To date, these are the only models that provide outputs for both GHG and NAT experiments.

CFSR (Saha et al. 2010), ERA-Interim (Dee et al. 2011) and the JRA-25 (Onogi et al. 2007), detailed in Table S2. These reanalyses were averaged with equal weighting to form an ensemble, following Wang et al. (2013). Other datasets included were the Extended Reconstructed Sea Surface Temperature (ERSST, v3b) derived from the International Comprehensive Ocean–Atmosphere Dataset (Smith and Reynolds 2003), and global precipitation produced by NOAA's Precipitation Reconstruction over Land (PREC/L) and historical observations over ocean (PREC/O); these commence from 1948 (Chen et al. 2002). The definition of ENSO was determined by the monthly mean Niño3.4 index provided by the Climate Prediction Center (CPC).

3. Results

a. El Niño factor

As shown in Fig. 1c, the May 2015 anomaly of the 250-hPa streamfunction (as a departure from the 1981-2010 mean) depicts a standing trough over the southwest U.S.; this trough directed a series of short-wave disturbances towards Texas and Oklahoma (not shown). The 850-hPa wind anomalies (vector) depict the intensified southerly flow that conveyed moisture from the Gulf of Mexico into the Great Plains; these upper- and lower-level features indicate a coupling of baroclinic (frontal) forcing and moisture supply, and are of climatological importance in sustaining late-spring rainfall in the southern Great Plains (Helfand and Schubert 1995; Higgins et al. 1997; Santanello et al. 2012). Additionally, as shown in Fig. 1c, the anomalous trough over the southwest U.S. was accompanied by a subtropical anticyclonic anomaly in the eastern Pacific; this formed a wave pattern that resembles the atmospheric response to equatorial eastern Pacific SST forcing (e.g., Mo 2010). Daily rainfall data over Texas and Oklahoma (not shown) indicated that the entire month of May, with the exception of

May 1st-3rd and 12th, experienced consecutively large rainfall totals. The coexistence of an El Niño with large May rainfall echoes the observation of Lee et al. (2014b) that a positive precipitation anomaly centered over Texas tends to occur in late spring during the onset of an El Niño; this is coincident with CPC's announcement of 2015's El Niño advisory in March (i.e. issued when El Niño conditions are observed and expected to build) so that by the time May came around, the warm-tongue SST pattern (Fig. 1a) had transitioned towards its onset phase.

To examine the long-term change in the relationship between the ENSO teleconnection and precipitation anomalies in the southern U.S. we regressed the May Niño-3.4 index with the monthly mean precipitation for two periods: 1948-1980 (Fig. 2a) and 1981-2014 (Fig. 2b). Here, all the data within either period were linearly detrended to minimize the effect of any interdecadal trends or cycles. While the east-west contrast between a wetter Great Plains and drier Southeast is apparent in both periods, the regressed precipitation over Texas and Oklahoma exhibits a distinctively stronger signal in the latter time period. Next, the role of increased GHG in the atmosphere in the ENSO-precipitation relationship was analyzed by conducting the regression analysis for CMIP5's NAT-only (Fig. 2c) and GHG-only (Fig. 2d) experiments, covering the period 1970-2005. Despite differences in the general precipitation pattern as compared to observations (a result of inherent model biases), the GHG-only forcing produces a significantly stronger precipitation response over Texas and Oklahoma. Moreover, a similar analysis performed using the CESM1 LEP data for the periods of 1940-1980 (Fig. 2e) and 2010-2050 (Fig. 2f; i.e., that reflects future precipitation outcomes) reveals the same tendency, i.e. stronger precipitation anomalies over Texas and Oklahoma in response to a transformational ENSO signature in a warmer climate. Noteworthy here is that, since CESM1 is not included in the 17 CMIP5 models, this result

also serves to validate the multi-model analysis. Since the regression is linear the corollary is valid – that is, the La Niña-induced precipitation deficit in the southern Great Plains would likewise result in Texas and Oklahoma and equally so, any overtones associated with a strong La Niña (Peterson et al. 2012). In the future, as can be inferred from Fig. 2f, one may anticipate the tendency for an increased ENSO impact on the southern Great Plains precipitation regime.

Recent research (Meehl and Teng 2007; Stevenson et al. 2012; Wang et al. 2015) indicates that ENSO teleconnection and accompanying regional impact would intensify in response to increasing SST. Under such a premise we regressed the 250-hPa streamfunction with the Niño-3.4 index (Fig. 3a) for the same two time periods as in Fig. 2. The ENSO-induced "great arch" teleconnection emanating from the central equatorial Pacific is visible in both periods. However, the post-1980 time period features a noticeably stronger circulation amplitude; this includes a deepened, standing trough west of Texas. The deepened trough, together with an abnormally strong subtropical jet that extends into Baja California (not shown), is indicative of enhanced synoptic forcing directed towards the southern Great Plains as was the case in May 2015. In Figs. 3c and 3d we show the tropical precipitation (shaded) and SST (contoured) regressions during the different time periods: After 1980, the El Niño-induced precipitation and SST anomalies reveal marked increases over the equatorial central Pacific – in fact, at the center (outlined by a yellow circle), precipitation has increased 1.7 times in the latter period while SST increased by about 1°C (Figs. 3e and 3f).

Focusing on wintertime, Zhou et al. (2014) found that the tropical Pacific precipitation anomalies associated with ENSO would intensify in a warmer climate while extending eastward over the equatorial eastern basin. Such an increase in precipitation, which is similar to what Fig. 3d shows, leads to substantial change in

latent heating that can further intensify the teleconnection response (e.g., Branstator 1985; Palmer 2014; Wang et al. 2015). To examine further, we conducted a comparable analysis to that of Fig. 3 but this time with respect to the CMIP5 models in order to detect any change in the ENSO teleconnection between that of NAT and GHG; this is shown in the Supplemental Figure (S1) for the time period 1970-2005. The results are alike in that, under CHG forcing, an intensified teleconnection wave train linked to a deepened trough in the southwestern U.S. is observed to be the case and is accompanied with precipitation anomaly enhancement over the equatorial central Pacific. Altogether, the results presented here (i.e. Figs. 2 and 3) as well as those in the current literature support the strengthening of the ENSO teleconnection due to a warmer climate.

b. Other factors

The cause of widespread flooding is manifold and cannot be explained solely by any single weather/climate process. Additional circulation features associated with the extreme rainfall of May 2015 do exist: By conducting a power spectral analysis for zonal wave numbers in the May 2015 streamfunction anomaly within the 30°-50°N latitudinal zone, a wave-2 regime and a wave-5 regime emerged (see Fig. S2). While the wave-2 regime reflects the ENSO-induced circulation anomaly that is inherently of longer wavelength (Wallace and Gutzler 1981), the wave-5 regime echoes an increasingly influential mode of the so-called circumglobal teleconnection (Branstator 2002; Schubert et al. 2011; Teng et al. 2013). Focusing on the latter, we performed a zonal harmonic analysis on the streamfunction anomaly following Wang et al. (2013); this wave-5 component is shown in Fig. 4a. A clear short-wave train emerges encompassing the deepened trough west of the flooded region and the anomalous ridge to the east. We next computed the linear trend (slope) of this wave-5 streamfunction for the time period of 1980-2014 from the ensemble of modern-era reanalyses; this is shown in Fig.

4b. The trend reveals a distinct wave pattern in the wave-5 regime and the phase of this intensified short-wave train is remarkably coincident with the May 2015 anomaly; this result suggests an intensification of the short-wave circulation and is resonant with the findings of Meehl and Teng (2007) and Lee et al. (2014a), i.e., that increased ENSO amplitude that ensues from a warmer climate produces a prominent wave-5 pattern within the teleconnection.

The similarity between the two wave-5 circulations (Figs. 4a and 4b) accompanied by a stronger low-level jet (LLJ) in the Great Plains (Fig. 1c) implies a coupling enhancement in the classic trough-LLJ setting (Uccellini 1980), and such coupling produces the majority of precipitation in the southern Great Plains during the late spring (Wang and Chen 2009). Readers are referred to Text S1 for further explanation of the relevant synoptic processes. The long-term change in this trough-LLJ coupling was further examined by computing the linear trend of the column water vapor fluxes ($\vec{Q}$), integrated up to 300 hPa (Fig. 4c). A distinct band of southerly $\vec{Q}$ forms over the southern Great Plains signifying an intensified LLJ that is coupled with the deepened upper-level trough to the west, as was noted in Barandiaran et al. (2013). While Weaver et al. (2009) related the springtime LLJ intensification to interdecadal variation in the North Atlantic, Cook et al. (2008) linked the increased LLJ with the anthropogenic global warming.

Though the cause of flood is not the focus here, a final comment that should be realized is that ground conditions in Texas more than likely were "preconditioned" to initiate flooding conditions (Jesse Meng, NOAA/NCEP/EMC, personal communication 2015): As Fig. S3 shows, April 2015 was abnormally wet in southern Texas (though not exceptionally) whereupon soil moisture in the Huston area was already above normal for that time of year which carried forward into early May near saturation conditions.

4. Summary

The record precipitation that occurred over Texas and Oklahoma during the month of May 2015 was the result of a series of climate interactions and anomalies. Foremost is the role that ENSO played: A developing El Niño has a tendency to increase spring precipitation over the southern Great Plains and this effect was found to have intensified since 1980; this intensification was concomitant with a warmer atmosphere due to anthropogenic GHG. Specifically, the intensified ENSO teleconnection appears to be triggered by enhanced latent heating in the equatorial central Pacific, and is associated with broad SST warming in the tropics. In essence, there was a detectable effect of anthropogenic global warming on the teleconnection and moisture transport leading to May 2015's high precipitation. Previous studies as well as this one point to the following processes: (1) long-term warming of the tropical Pacific acting to strengthen the atmospheric response to ENSO; (2) El Niño modulating the wave-5 circulation pattern in a warmer climate and its phase-lock with the May 2015 anomaly; (3) enhancement of the Great Plains LLJ and associated moisture supply in late spring; and (4) the LLJ's coupling with the deepened spring trough at upper levels. All the aforementioned processes together with the attribution analyses of CMIP5 and CESM1 models analyzed here point toward the exacerbating effect of increasing GHG on the springtime precipitation over Texas and Oklahoma during a developing El Niño – this being so currently (i.e. 2015) and in the future. Furthermore, the diagnostic analyses detailed here, in which increased extreme events and a warmer climate were shown to be dynamically linked, is key in the provision of seasonal predictions as a guide to future occurrences and intensities of extreme weather events.

Acknowledgement

Soil moisture information shared by Jesse Meng is appreciated. ENSO indices are provided by the CPC at http://www.cpc.ncep.noaa.gov/data/indices/sstoi.indices. All data utilized in this study are freely available from the following sources: the NOAA/OAR/ESRL PSD, Boulder, Colorado, USA, from their Web site at http://www.esrl.noaa.gov/psd/, the CMIP5 Data Portal at http://cmip-pcmdi.llnl.gov/cmip5/data_portal.html, and the CESM1 Large Ensemble Community Project at http://www.cesm.ucar.edu/experiments/cesm1.1/LE/.

References:

Barandiaran, D., S.-Y. Wang, and K. Hilburn, 2013: Observed trends in the Great Plains low-level jet and associated precipitation changes in relation to recent droughts. *Geophy. Res. Lett.*, **40,** 2013GL058296.

Branstator, G., 1985: Analysis of General Circulation Model Sea-Surface Temperature Anomaly Simulations Using a Linear Model. Part I: Forced Solutions. *J. Atmos. Sci.*, **42,** 2225-2241.

——, 2002: Circumglobal Teleconnections, the Jet Stream Waveguide, and the North Atlantic Oscillation. *J. Climate*, **15,** 1893-1910.

Chen, M., P. Xie, J. E. Janowiak, and P. A. Arkin, 2002: Global Land Precipitation: A 50-yr Monthly Analysis Based on Gauge Observations. *Journal of Hydrometeorology*, **3,** 249-266.

Cook, K. H., E. K. Vizy, Z. S. Launer, and C. M. Patricola, 2008: Springtime Intensification of the Great Plains Low-Level Jet and Midwest Precipitation in GCM Simulations of the Twenty-First Century. *J. Climate*, **21,** 6321-6340.

Dee, D. P., and Coauthors, 2011: The ERA-Interim reanalysis: configuration and performance of the data assimilation system. *Quarterly Journal of the Royal Meteorological Society*, **137,** 553-597.

Helfand, H. M., and S. D. Schubert, 1995: Climatology of the Simulated Great Plains Low-Level Jet and Its Contribution to the Continental Moisture Budget of the United States. *J. Climate*, **8,** 784-806.

Higgins, R., Y. Yao, E. Yarosh, J. E. Janowiak, and K. Mo, 1997: Influence of the Great Plains low-level jet on summertime precipitation and moisture transport over the central United States. *J. Climate*, **10,** 481-507.

Kalnay, E., and Coauthors, 1996: The NCEP/NCAR 40-Year Reanalysis Project. *Bull. Amer. Meteor. Soc.*, **77,** 437-471.

Kay, J. E., and Coauthors, 2014: The Community Earth System Model (CESM) Large Ensemble Project: A Community Resource for Studying Climate Change in the Presence of Internal Climate Variability. *Bull. Amer. Meteor. Soc.*

Lee, J.-Y., B. Wang, K.-H. Seo, J.-S. Kug, Y.-S. Choi, Y. Kosaka, and K.-J. Ha, 2014a: Future Change of Northern Hemisphere Summer Tropical–Extratropical Teleconnection in CMIP5 Models*. *J. Climate*, **27,** 3643-3664.

Lee, S.-K., B. E. Mapes, C. Wang, D. B. Enfield, and S. J. Weaver, 2014b: Springtime ENSO phase evolution and its relation to rainfall in the continental U.S. *Geophy. Res. Lett.*, **41,** 2013GL059137.

Meehl, G. A., and H. Teng, 2007: Multi-model changes in El Niño teleconnections over North America in a future warmer climate. *Clim. Dynamics*, **29,** 779-790.

Meehl, G. A., and Coauthors, 2014: Decadal Climate Prediction: An Update from the Trenches. *Bull. Amer. Meteor. Soc.*, **95,** 243-267.

Mo, K. C., 2010: Interdecadal Modulation of the Impact of ENSO on Precipitation and Temperature over the United States. *J. Climate*, **23,** 3639-3656.

Onogi, K., and Coauthors, 2007: The JRA-25 Reanalysis. *Journal of the Meteorological Society of Japan. Ser. II*, **85,** 369-432.

Palmer, T., 2014: Record-breaking winters and global climate change. *Science*, **344,** 803-804.

Peterson, T. C., P. A. Stott, and S. Herring, 2012: Explaining extreme events of 2011 from a climate perspective. *Bull. Amer. Meteor. Soc.*, **93,** 1041-1067.

Rienecker, M. M., and Coauthors, 2011: MERRA - NASA's Modern-Era Retrospective Analysis for Research and Applications. *J. Climate***,** in press.

Ropelewski, C. F., and M. S. Halpert, 1986: North American precipitation and temperature patterns associated with the El Niño/Southern Oscillation (ENSO). *Mon. Wea. Rev.*, **114,** 2352-2362.

Ropelewski, C. F., and M. S. Halpert, 1987: Global and Regional Scale Precipitation Patterns Associated with the El Niño/Southern Oscillation. *Mon. Wea. Rev.*, **115,** 1606-1626.

Saha, S., and Coauthors, 2010: The NCEP Climate Forecast System Reanalysis. *Bull. Amer. Meteor. Soc.*, **91,** 1015-1057.

Santanello, J. A., C. D. Peters-Lidard, A. Kennedy, and S. V. Kumar, 2012: Diagnosing the Nature of Land–Atmosphere Coupling: A Case Study of Dry/Wet Extremes in the U.S. Southern Great Plains. *Journal of Hydrometeorology*, **14,** 3-24.

Schubert, S., H. Wang, and M. Suarez, 2011: Warm season subseasonal variability and climate extremes in the Northern Hemisphere: The role of stationary Rossby waves. *J. Climate*, **24,** 4773–4792.

Smith, T. M., and R. W. Reynolds, 2003: Extended Reconstruction of Global Sea Surface Temperatures Based on COADS Data (1854-1997). *J. Climate*, **16,** 1495-1510.

Stevenson, S., B. Fox-Kemper, M. Jochum, R. Neale, C. Deser, and G. Meehl, 2012: Will there be a significant change to El Niño in the twenty-first century? *J. Climate*, **25,** 2129-2145.

Taylor, K. E., R. J. Stouffer, and G. A. Meehl, 2011: An Overview of CMIP5 and the Experiment Design. *Bull. Amer. Meteor. Soc.*, **93,** 485-498.

Teng, H., G. Branstator, H. Wang, G. A. Meehl, and W. M. Washington, 2013: Probability of US heat waves affected by a subseasonal planetary wave pattern. *Nature Geoscience*, **6,** 1056-1061.

Uccellini, L. W., 1980: On the Role of Upper Tropospheric Jet Streaks and Leeside Cyclogenesis in the Development of Low-Level Jets in the Great Plains. *Mon. Wea. Rev.*, **108,** 1689-1696.

Wallace, J. M., and D. S. Gutzler, 1981: Teleconnections in the Geopotential Height Field during the Northern Hemisphere Winter. *Mon. Wea. Rev.*, **109,** 784-812.

Wang, S.-Y., and T.-C. Chen, 2009: The Late-Spring Maximum of Rainfall over the U.S. Central Plains and the Role of the Low-Level Jet. *J. Climate*, **22,** 4696-4709.

Wang, S.-Y., R. E. Davies, and R. R. Gillies, 2013: Identification of extreme precipitation threat across midlatitude regions based on short-wave circulations. *Journal of Geophysical Research: Atmospheres*, **118,** 2013JD020153.

Wang, S.-Y., W.-R. Huang, and J.-H. Yoon, 2015: The North American winter 'dipole' and extremes activity: A CMIP5 assessment. *Atmospheric Science Letters***,** in press.

Wang, S.-Y., L. Hipps, R. R. Gillies, and J.-H. Yoon, 2014: Probable causes of the abnormal ridge accompanying the 2013–2014 California drought: ENSO precursor and anthropogenic warming footprint. *Geophy. Res. Lett.*, **41,** 2014GL059748.

Weaver, S. J., S. Schubert, and H. Wang, 2009: Warm Season Variations in the Low-Level Circulation and Precipitation over the Central United States in Observations, AMIP Simulations, and Idealized SST Experiments. *J. Climate*, **22,** 5401-5420.

Zhou, Z.-Q., S.-P. Xie, X.-T. Zheng, Q. Liu, and H. Wang, 2014: Global Warming–Induced Changes in El Niño Teleconnections over the North Pacific and North America. *J. Climate*, **27,** 9050-9064.

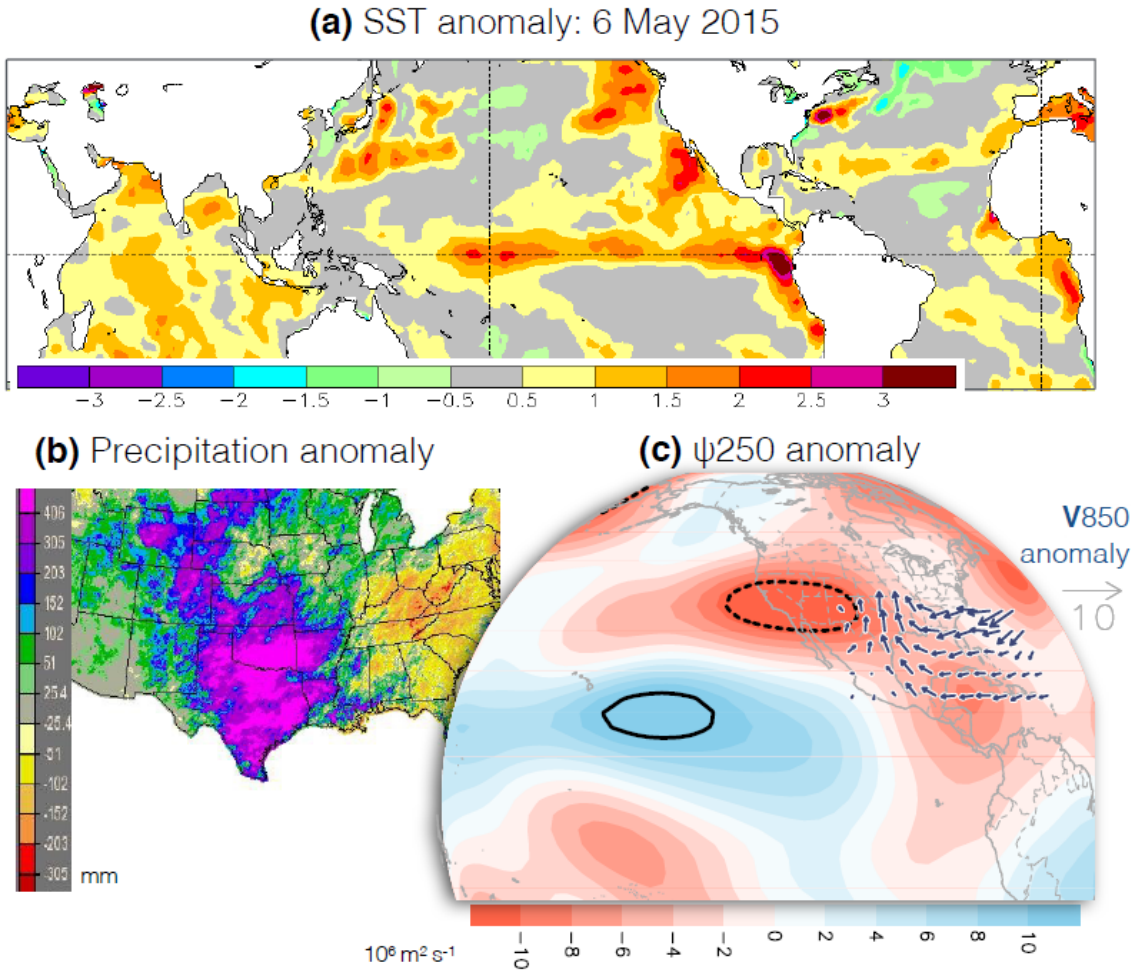

Fig. 1 (a) SST anomaly (°C) of May 6-15, 2015 obtained from http://www.ospo.noaa.gov/Products/ocean/sst/anomaly/. (b) May 2015 precipitation anomaly in mm obtained from http://water.weather.gov/precip/. (c) 250-hPa streamfunction anomaly (ψ; shadings) and 850-hPa anomalous winds (vectors, m/s) of May 2015 derived from NCEP1 Reanalysis; the black contours outline $\pm 12 \times 10^6$ m^2 s^{-1}.

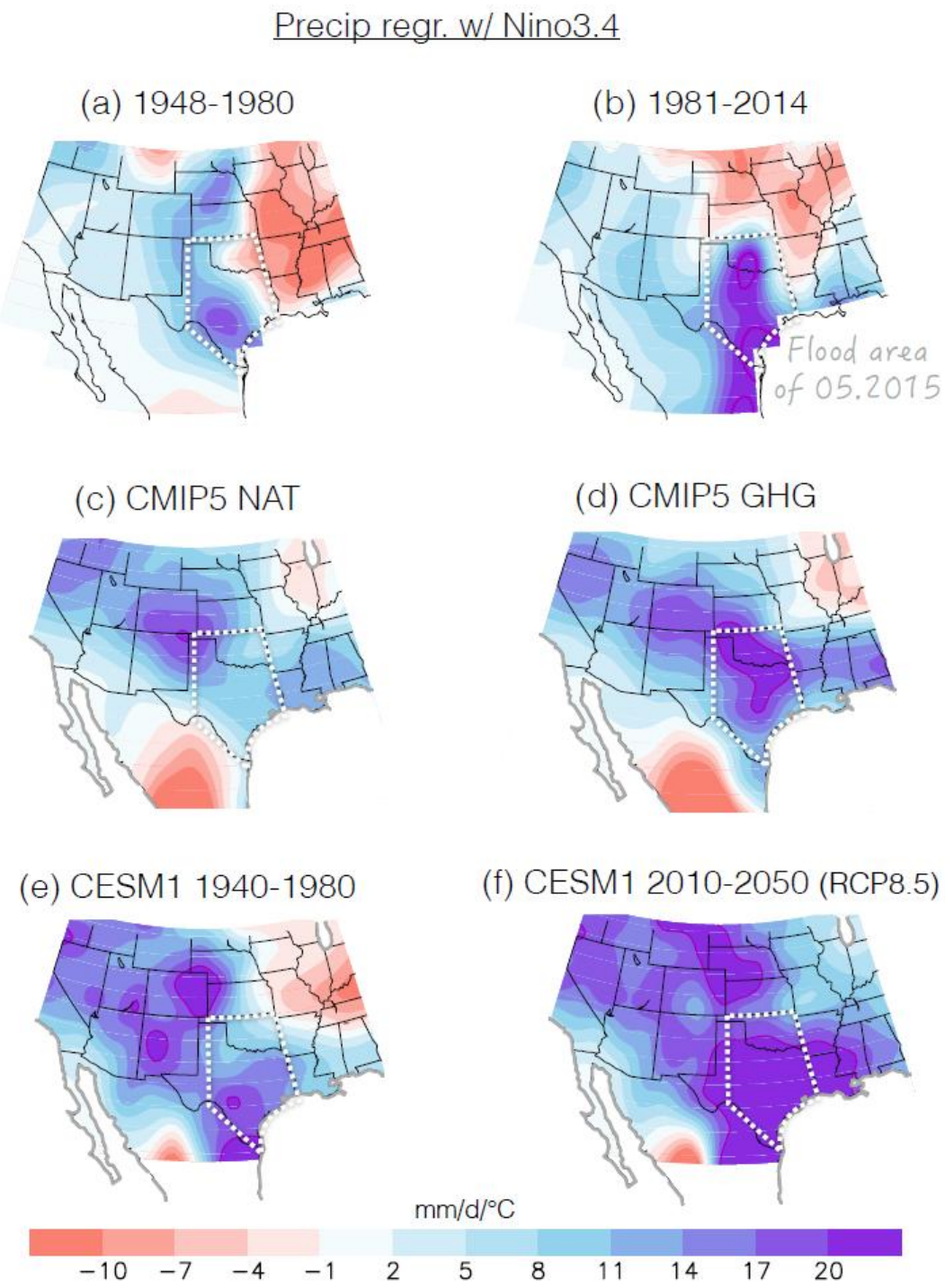

Fig. 2 May precipitation regression with Nino-3.4 index for (a) 1948-1980 and (b) 1981-2014; values exceeding ± 9 are significant at the 95% interval. The high precipitation region in Texas and Oklahoma is outlined with the white dashed line. (c) and (d) Same as (a) and (b) except for the ensembles of CMIP5 historical experiments from the NAT-only and GHG-only forcing experiments, respectively, over the 1970-2005 period. Purple contours outline the values of 23. (e) and (f) Similar to (c) and (d) except for the 30-member ensembles of CESM1 for the1940-1980 and 2010-2050 periods, respectively.

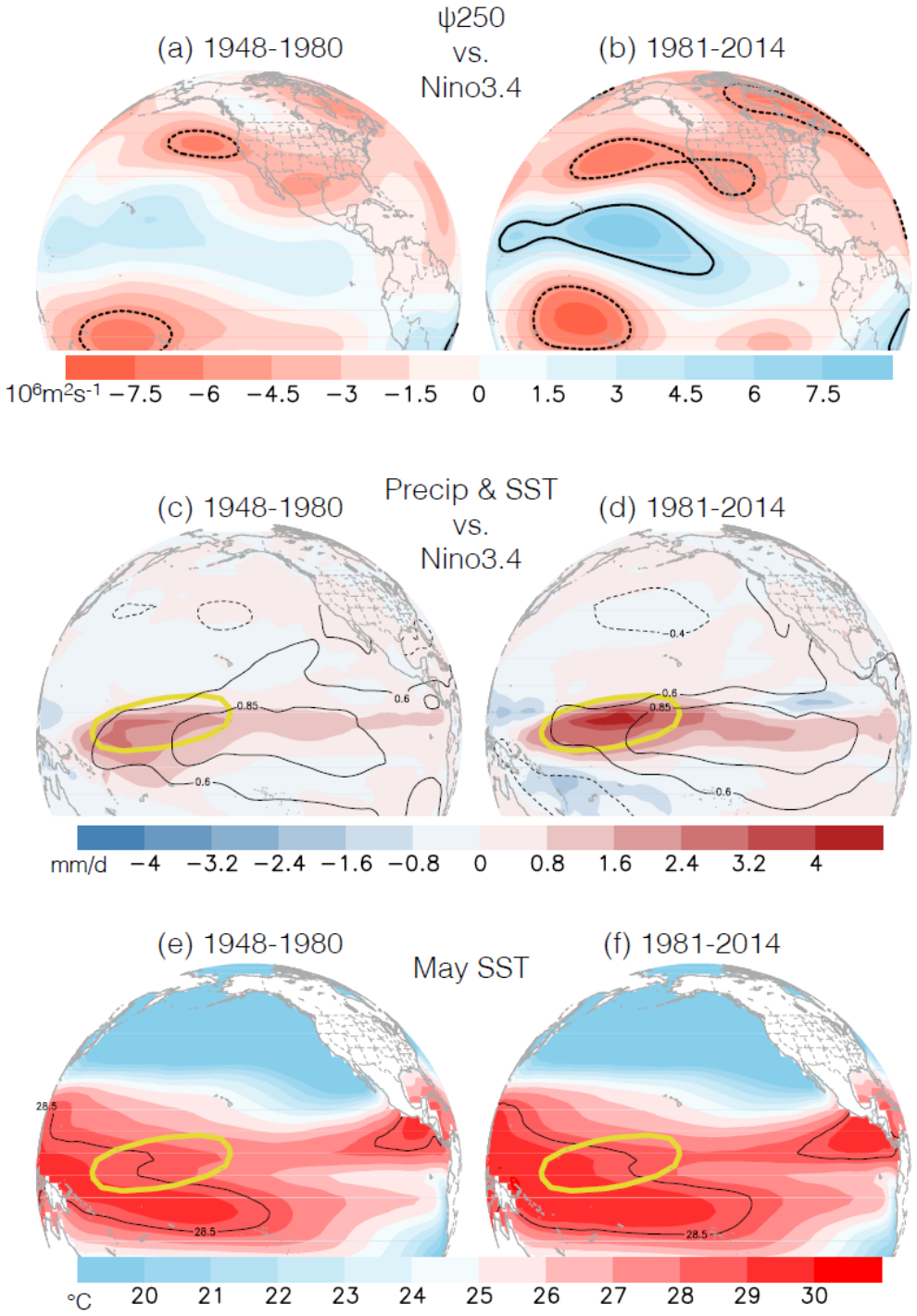

Fig. 3 Same as Figs. 2a and 2b except for (a, b) the observed 250-hPa streamfunction anomalies ψ (contours for +/- 5), and (c, d) global precipitation (shadings) and SSTA (contours for -0.4, 0.6, and 0.85°C) in May. Here the Nino-3.4 index was standardized so the variables reflect their native unit. (e) and (f) May SST means of the two periods with a single contour of 28.5°C encircling the warm pool. The yellow ovals indicate the precipitation anomaly center based upon the 1981-2014 period. Contours in (a, b) outline 5×10^6 m^2 s^{-1} which cover the 99% confidence interval.

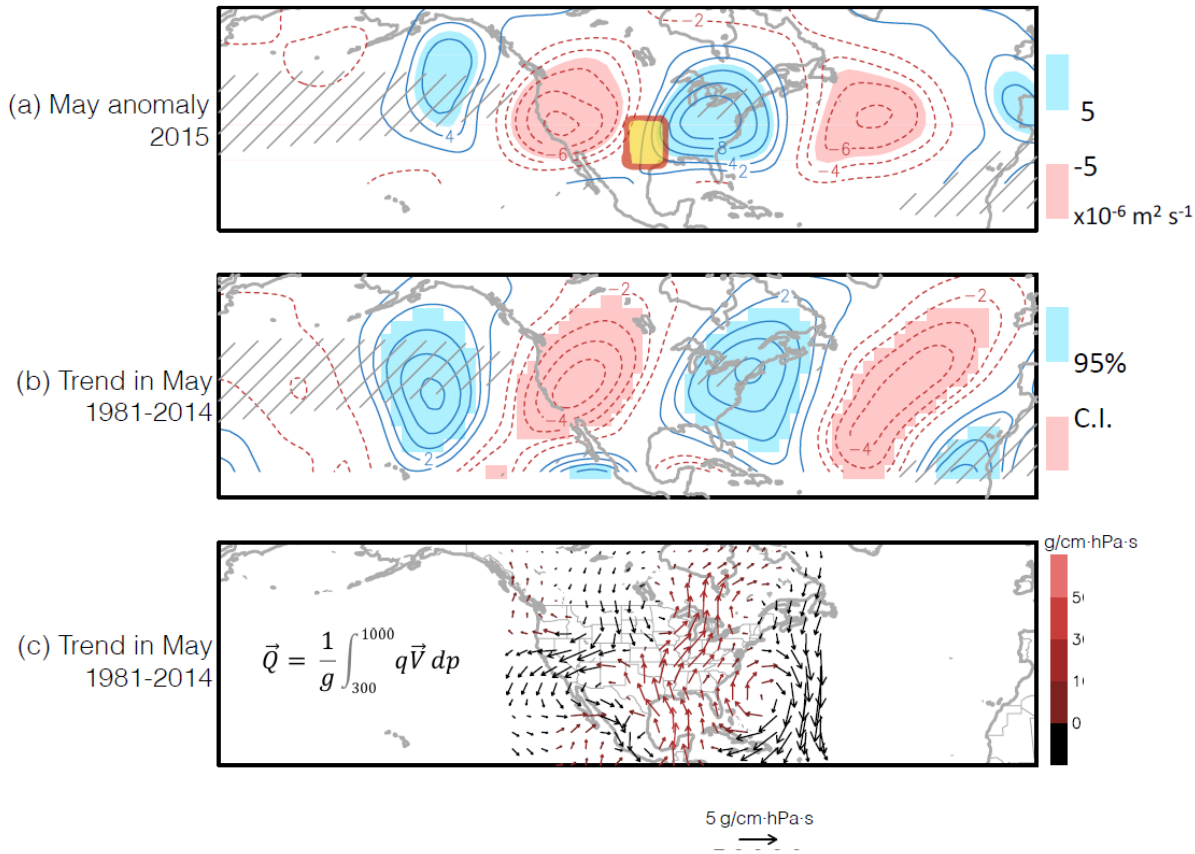

Fig. 4 (a) The 250 hPa streamfunction anomalies of May 2015 in the wave-5 regime overlaid with the climatological jet stream (hatched; |V| > 25 m/s); the yellow-red domain indicates the Texas-Oklahoma floods. (b) Linear trend (total change over the1981-2014 period) of the wave-5 regime streamfunction (unit: $10^6\,m^2\,s^{-1}$) computed from the ensemble of four satellite-era reanalyses, with the 95% confidence interval shaded. Notice the phase coincidence between (a) and (b). (c) Same as (b) but for the column water vapor flux (formula indicated, where g is gravity, q is specific humidity, p is pressure and **V** is horizontal winds). Southerly component is colored with the red scale.

SOM

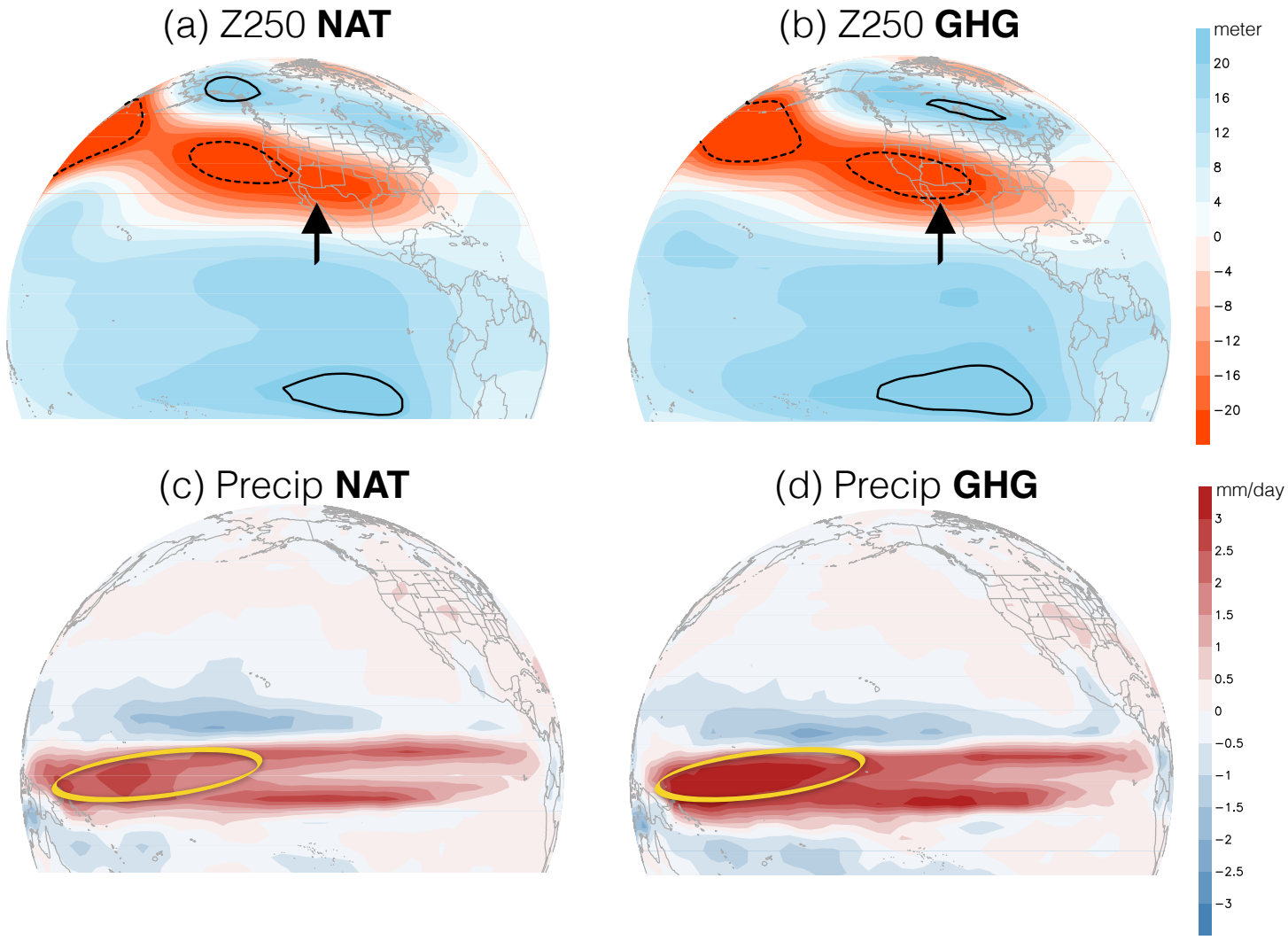

↑

Same as Figs. 3a and 3c except for the May 250-hPa geopotential height and global precipitation anomalies derived from the CMIP5 ensemble of NAT and GHG. Coutures are +/- 25 m. Notice the anomalous trough in the western U.S. (arrow indicated) and the stronger precipitation in GHG (outlined)that is stronger in GHG than in NAT. The Nino-3.4 index was standardized so the variables reflect their native unit.

SOM

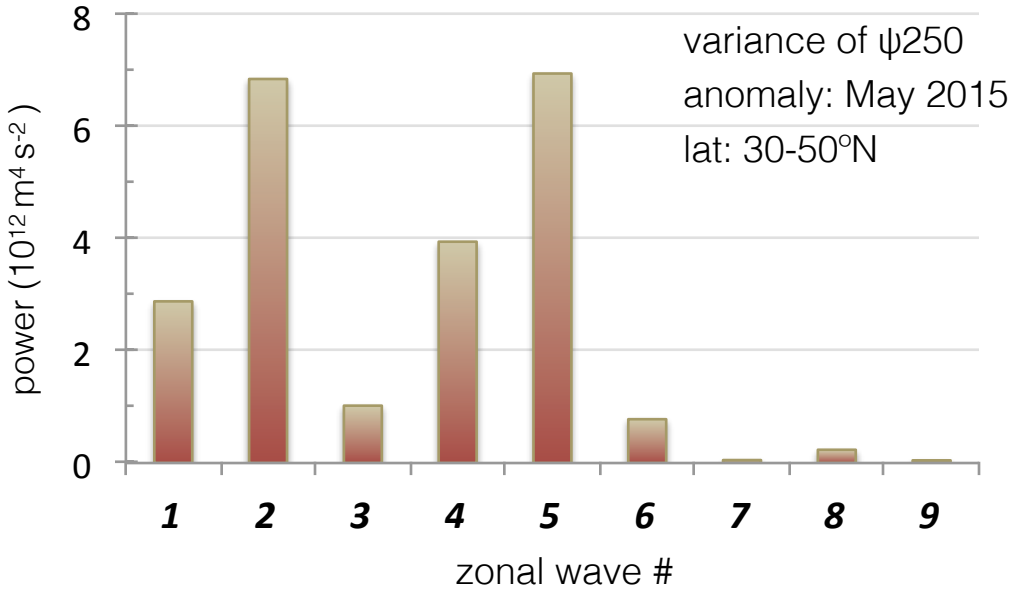

←
Power spectral analysis of the zonal wave regimes in the 250-hPa streamfunction anomaly of May 2015, averaged within the 30°-50°N latitude zone. Note the wave-5 power.

SOM

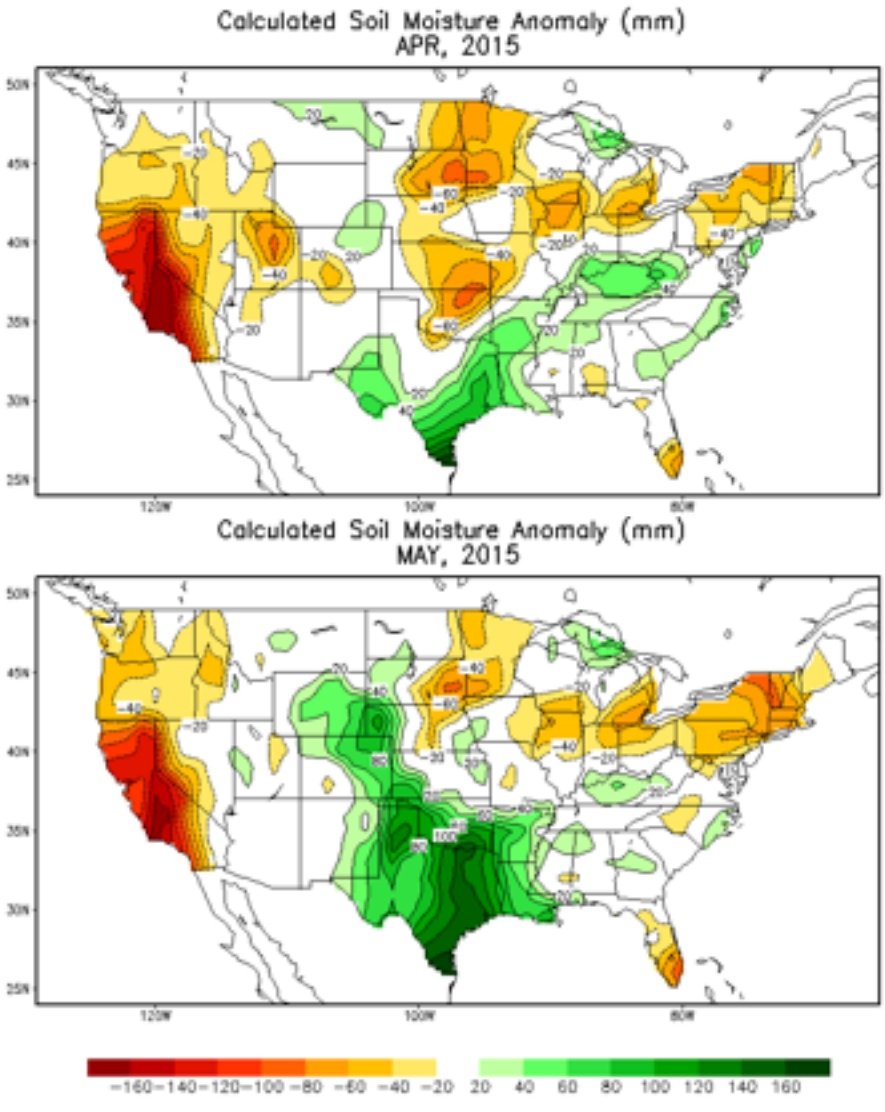

←
Soil moisture anomaly provided by the NCEP Climate Prediction Center for (top) April 2015 and (bottom) May 2015. Notice the Texas area.

Online Supplementary Material (SOM)

Precipitation

250-hPa streamfunction

(a) April 2015 anomaly

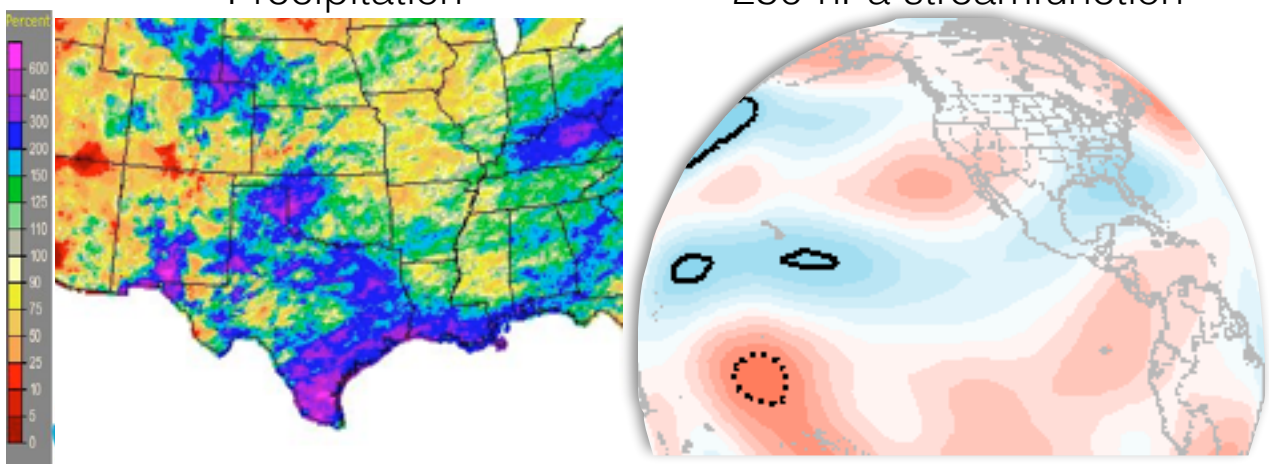

1948-1980

1981-2014

(b) April regression of Precipitation with Nino-3.4

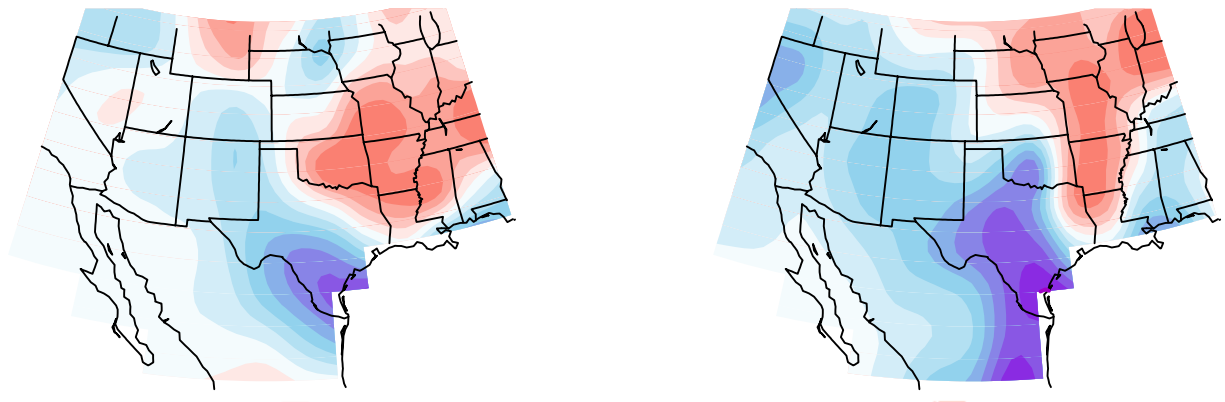

(c) April regression of 250-hPa streamfunction with Nino-3.4

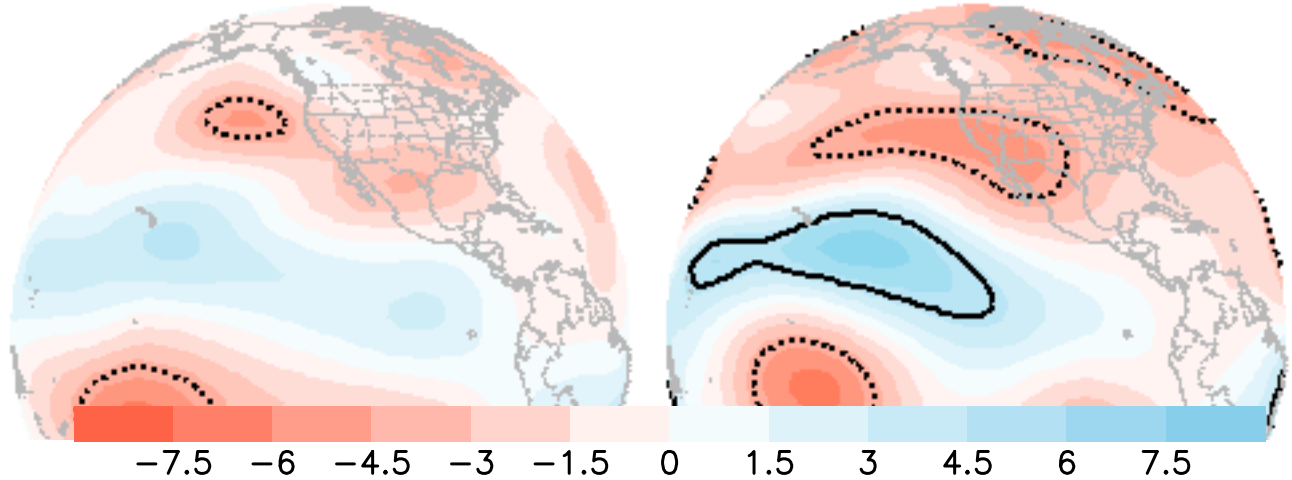

(d) April regression of SSTA (contours) and precipitation (shadings) with Nino-3.4

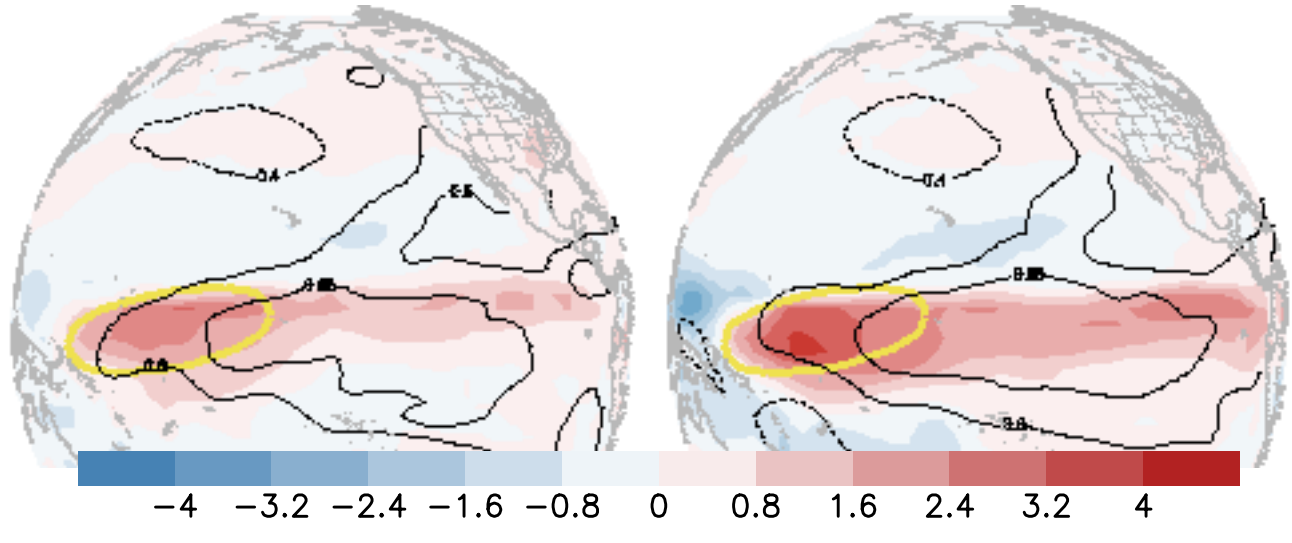

SOM: Same as Figs. 1-3 including units and color scale, except for the month of April.